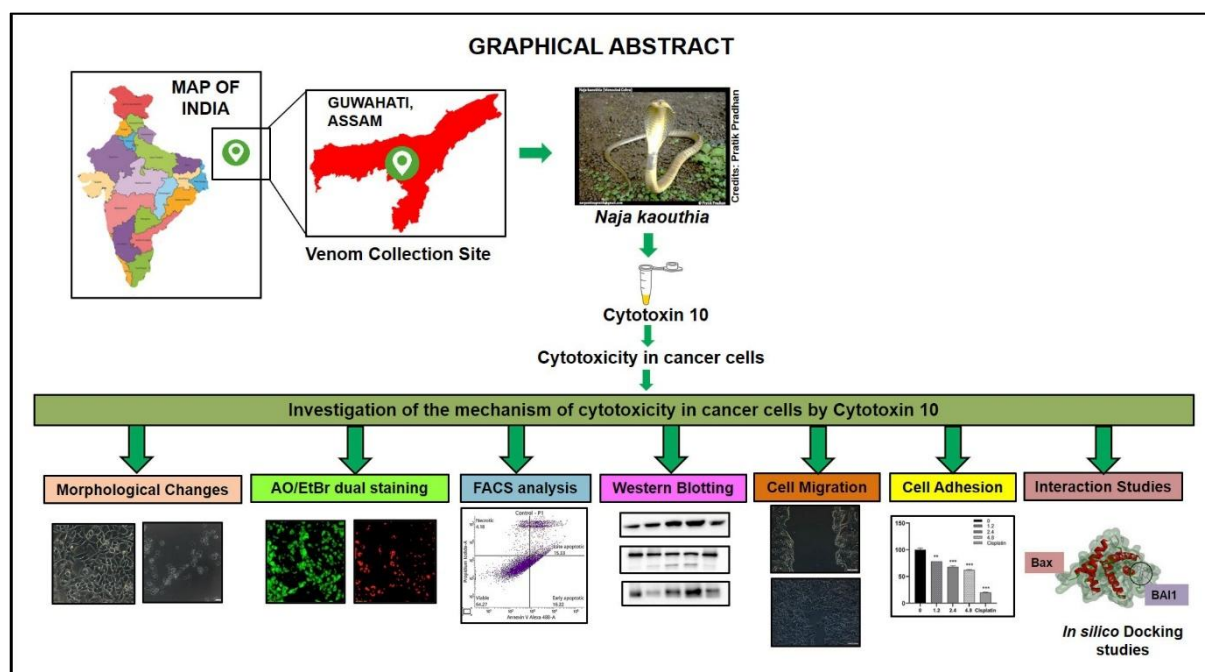


CHAPTER 5

Understanding the mechanism of cytotoxic activity of Cytotoxin 10

Chapter 5: Understanding the mechanism of cytotoxic activity of Cytotoxin 10



5.1 Introduction

In the previous chapter, the cytotoxicity of peak P9 from *N. kaouthia* venom was studied on breast and lung cancer cell lines and further P9 was identified as Cytotoxin 10. The first record of antitumor cytolytic activity of cytotoxins was provided by Zaheer et al. where it was reported that cytotoxin P6 from *N. naja* venom could actively lyse Yoshida sarcoma cells [319]. Subsequently, other studies have elaborated the strong cytolytic activity of cytotoxins on tumor cells compared to normal cells (spleen cells, peritoneal exudate cells or erythrocytes) [320]. The cytotoxin P4 from *N. nigricollis* venom also exhibited preferential cytotoxicity for tumor cells, however, the radioactive P4 exhibited binding dependencies to melanoma and leukemic cells on factors such as temperature, concentration and incubation time [321]. Detailed study of the mechanism of action of cytotoxins on cancer cells revealed two main pathways of cell death, namely necrosis

which is mediated by lysosomal damage, and apoptosis which involves various apoptotic proteins and signaling mediators [322].

This chapter elucidates the mechanism of cytotoxic activity of Cytotoxin 10 purified from *N. kaouthia* venom of North-East India origin against the breast (MCF-7) and lung (A549) cancer cell lines. The expression of apoptotic proteins Bax, Bcl-2, caspase-7 and PARP after Cytotoxin 10 treatment of cancer cells were also investigated. The effect of Cytotoxin 10 on migration and adhesion of cancer cells, the two key signature parameters of metastasis was also studied. Furthermore, the interaction of Cytotoxin 10 with apoptosis related proteins was deciphered using *in silico* docking experiments.

5.2 Materials

5.2.1 Chemical and reagents

FBS was purchased from Gibco, USA. DMEM, Trypsin-EDTA, Penicillin-Streptomycin and Mitomycin were purchased from HiMedia, India. Collagen IV, Acridine orange and Doxorubicin were purchased from Sigma Aldrich, USA. Alexa FluorTM 488 Ready Flow Reagent was purchased from Invitrogen (Thermo Fisher Scientific, USA). Antibodies were procured from Cell Signalling Technology, USA. ECL substrate was purchased from Bio-Rad, USA.

5.2.2 Cell culture

MCF-7 (breast cancer) and A549 (lung cancer) cell lines were purchased from NCCS, Pune, India.

5.3 Methods

5.3.1 Morphological changes

Cells were seeded in a 96-well plate and upon 90% confluency, treated with different doses (5, 10 and 20 µg/ml) of Cytotoxin 10 and left for incubation for 24 and 48 hours. Morphological changes were observed under an inverted microscope (Olympus IX83).

5.3.2 AO/EtBr staining

Cells were seeded in a 96-well plate and incubated overnight. Following incubation, the cells were treated with different concentrations of Cytotoxin 10 (1.2, 2.4 and 4.8 µg/ml) for 48 hours. Then 4 µl of AO (100 µg/ml) and 4 µl of EtBr solution (100 µg/ml) each dissolved in PBS (1X PBS solution made up of 10 mM Na₂HPO₄, 137 mM NaCl, 2.7 mM KCl and 1.8 mM KH₂PO₄), pH 7.4 and mixed at 1:1 ratio, added for 5 min in dark followed by washing with PBS. Cells were visualized after 5-10 min of staining at 20X magnification. Images were taken from random fields for each treatment using a fluorescence microscope (Model Olympus IX83, Japan).

5.3.3 Annexin V-Alexa Fluor 488/PI binding study

Cells were seeded in a 24-well plate at the density of 0.50×10^6 cells per well and left for overnight incubation. Cells were treated with different concentrations (1.2, 2.4 and 4.8 µg/ml) of Cytotoxin 10 for 48 hours. After the completion of treatment, media was removed and cells were washed with ice cold PBS solution. Trypsin treatment was given for 2 min to detach the adherent cells. Media was added in equal amount as trypsin to neutralize the effect of trypsin. After harvesting, the cells were centrifuged and supernatant was decanted. Pellet was resuspended in 400 µl annexin binding buffer (1X). Annexin V (16 µl), Alexa FluorTM 488 Ready Flow Reagent and Propidium iodide (PI) (2 µg/ml) were added to each sample and incubated for 15 min. Samples were then proceeded with flow cytometry analysis as it allows the cells to be discriminated into four groups, namely viable (Annexin V⁻/PI⁻), early apoptosis (Annexin V⁺/PI⁻), late apoptosis (Annexin V⁺/PI⁺) and necrotic (Annexin V⁻/PI⁺) cells.

5.3.4 Western blot analysis

Cells were seeded in a 60 mm dish (2.5×10^6 cells) and incubated overnight. Cells were then treated with increasing concentrations (1.2 µg/ml, 2.4 µg/ml and 4.8 µg/ml) of Cytotoxin 10 for 24 hours. Treated cells were then lysed and proteins were extracted with ice cold RIPA buffer (Thermo Scientific, USA) which contains protease and phosphatase inhibitor cocktail. Equal amount of protein lysate from experimental samples (control and Cytotoxin 10 treated cells) were run in SDS-PAGE (12.5% Tris-Glycine) gel under reduced conditions and proteins were transferred to a PVDF

membrane using wet electrophoresis transfer unit (Bio-Rad Mini Trans-Blot cell) at 150 mA. The immunoblot was then immersed in blocking buffer (5% Skimmed milk in TBS-Tween 20) for 1-2 hours. The membrane was then washed in TBST and probed with primary antibody (1:1000 dilutions) overnight at 4 °C. Further, the membrane was washed with blocking buffer and incubated with corresponding secondary antibodies for 1 hour at room temperature. The blots were then incubated with chemiluminescence ECL substrate (Cat. No. 1705060, Bio-Rad, USA) and bands were visualized using Chemidoc XRS+ imaging system (Bio-Rad, USA). Quantification of the bands was done using GraphPad PRISM Software v. 8.4.2 (679).

5.3.5 Cell migration assay

Cells were seeded in 6-well plate upto 90% confluency and incubated for 6 hours in serum-free media. Cells were then treated with Mitomycin C (1 mg/ml) for 1 hour to stop proliferation. Straight scratches were given with a sterile tip. The cells were treated with desired concentrations (0.6µg/ml and 1.2 µg/ml) of Cytotoxin 10. Images were taken from five random fields at different time points (0 hour, 24 hours and 48 hours) for each of the samples using a fluorescence microscope (Model Olympus IX83, Japan). The area of the wound from these time points were measured using ImageJ software and recorded.

5.3.6 Cell adhesion assay

Cells were seeded in each well of a 6-well plate (5×10^5 cells) and treated with different doses of Cytotoxin 10 (1.2 µg/ml, 2.4 µg/ml and 4.8 µg/ml) in serum free media for 48 hours. Then the cells were trypsinized and resuspended in 1 ml of 1% BSA containing DMEM. Cell suspensions (200 µl, ~100,000 cells) were plated in 96-well plates precoated with collagen IV. Cells were allowed to adhere for 60 min and nonadherent cells were washed off with sterile PBS. The adhered cells were quantified using MTT assay as described earlier.

5.3.7 Interaction studies of Cytotoxin 10 and apoptotic proteins

Preparation of target proteins and ligands:

SWISS-MODEL server was employed to predict the three-dimensional structure of the snake protein Cytotoxin 10 [323]. The stereochemical parameters of the predicted model were analyzed with PROCHECK for further validation [324]. The RCSB Protein Data Bank (<https://www.rcsb.org/pdb/home/home.do>) was used to retrieve the three-dimensional structures of *Homo sapiens* proteins Bax (PDB ID: 1F16), Bcl-2 (PDB ID: 7YB7), PARP1 (PDB ID: 7KK4), and caspase-7 (PDB ID: 4FDL). Energy minimization of the protein structures were performed using the YASARA web server [325]. The structures of the selected inhibitors, namely BAI1, S55746, Olaparib, and DICA, were retrieved from PubChem (<https://pubchem.ncbi.nlm.nih.gov/>) database. and were converted to PDB format by UCSF Chimera version 1.17.1 [326]. The protein and ligand preparation for molecular docking and the visualization across various stages of docking were performed using UCSF Chimera.

Active binding site prediction:

Prediction of the active sites for the protein structures were carried out through the Computed Atlas of Surface Topography of Proteins (CASTp) (<http://cast.engr.uic.edu>). [327]. CASTp assesses the active site, pocket dimensions, and volume of the protein binding pocket. The binding sites for Bax, Bcl-2, PARP-1, and caspase-7 were predicted with surface areas of 428.403 Å², 382.723 Å², 2641.878 Å², and 618.752 Å², and volumes of 217.863 Å³, 194.126 Å³, 3675.870 Å³, and 364.984 Å³, respectively.

Molecular docking:

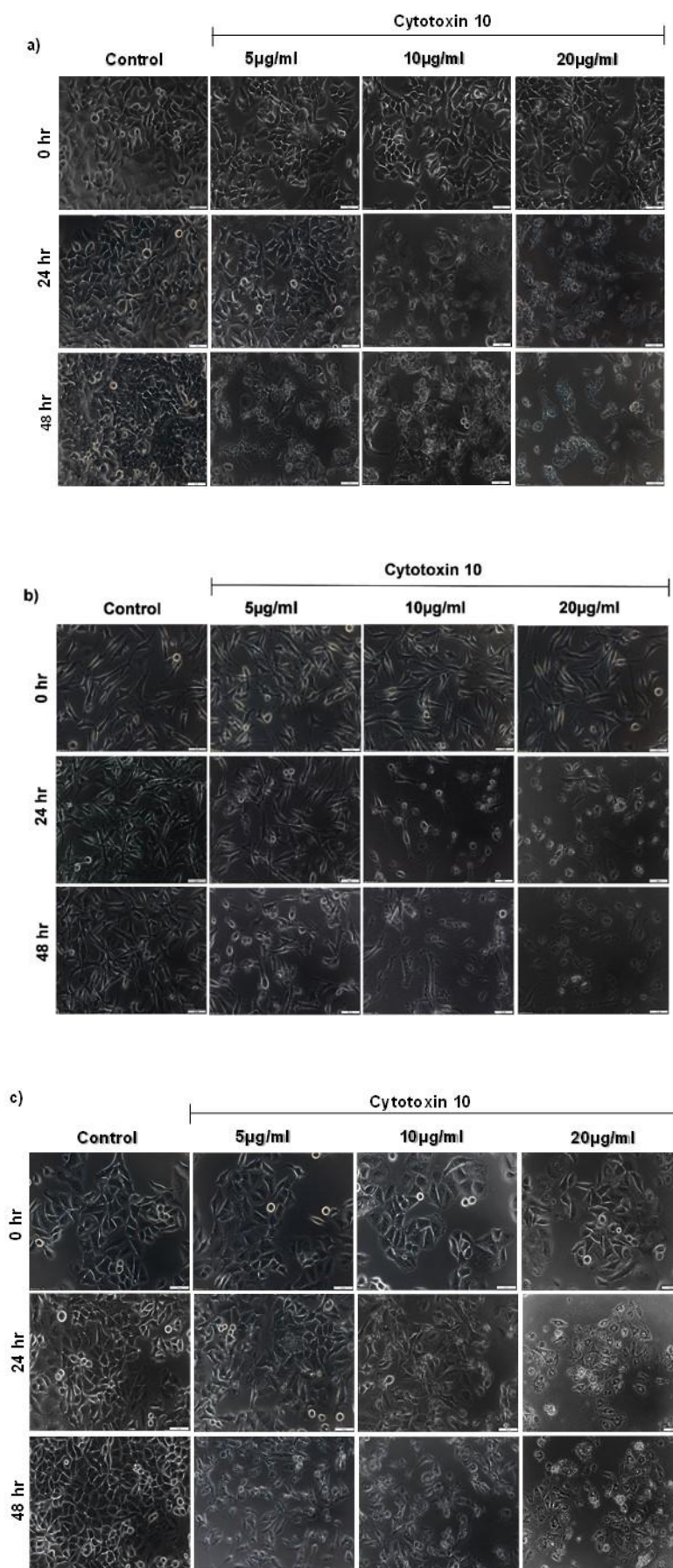
Docking studies for the target proteins with Cytotoxin 10 and with inhibitors were carried out utilizing the HADDOCK 2.4 and HDock web servers [328,329]. The easy interface segment of the HADDOCK 2.4 server was utilized to upload the structures of proteins and protein/ligands, with molecule-1 and molecule-2 assigned accordingly. The active sites identified by the CASTp server were subsequently specified. For every docking simulation, the cluster exhibiting the best HADDOCK score was selected. Similarly, the HDock server was used to upload receptor and ligand molecules. The active sites identified by CASTp were indicated under the advanced options. The most

optimal docked conformation was chosen according to HDOCK docking scores. LigPlot+ version 2.2.4 was used to prepare illustrations of binding poses generated by HADDOCK and HDOCK servers for protein-protein and protein-ligand interaction plots [330].

5.4 Results

5.4.1 Morphological changes

Distinct morphological changes of breast cancer (MCF-7 and MDA-MB-231) and lung cancer (A549 and NCI-H522) cells lines were observed after treatment with Cytotoxin 10 (5 µg/ml, 10 µg/ml and 20 µg/ml) for 24 and 48 hours. Treatment led to morphological abnormalities, such as, loss of structural integrity, cellular debris and loss of adhesion, which can also be co-related to a concentration-dependent reduction in the number of viable cells upon treatment with Cytotoxin as observed in previous chapter (Figure 4.13).



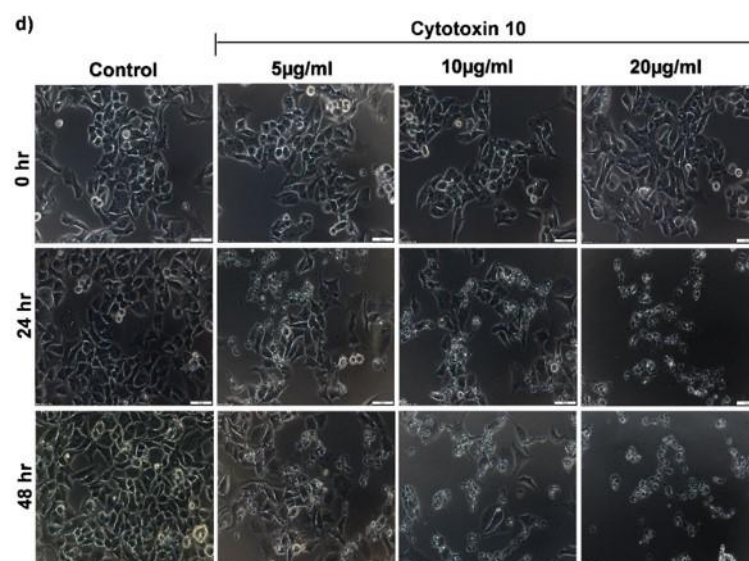


Figure 5.1: Brightfield images of a) MCF-7, b) MDA-MB-231, c) A549 and d) NCI-H522 after 24 and 48 hours of incubation with Cytotoxin 10 showing distinct morphological changes. Morphological changes were observed under an inverted microscope (Olympus IX83).

5.4.2 Induction of apoptosis by Cytotoxin 10

5.4.2.1 AO/EtBr staining

To understand the mechanism of cell death by Cytotoxin 10, apoptosis assay was performed in MCF-7 and A549 cells. AO/EtBr assay suggested that treatment with Cytotoxin 10 induced dose-dependent increase in apoptosis in both the cells. Treatment with 1.2, 2.4 and 4.8 µg/ml Cytotoxin 10 resulted in 16%, 66% and 80% increase in apoptotic cells in MCF-7 cells (Figure. 5.2a). Similar treatment in A549 cells resulted 47.89%, 62.69% and 78.23% increase in apoptotic cells (Figure. 5.2b). Doxorubicin (1 µg/ml) treated cells were used as positive control for the study. This observation was supported by flow cytometry analysis of Cytotoxin 10-treated cells.

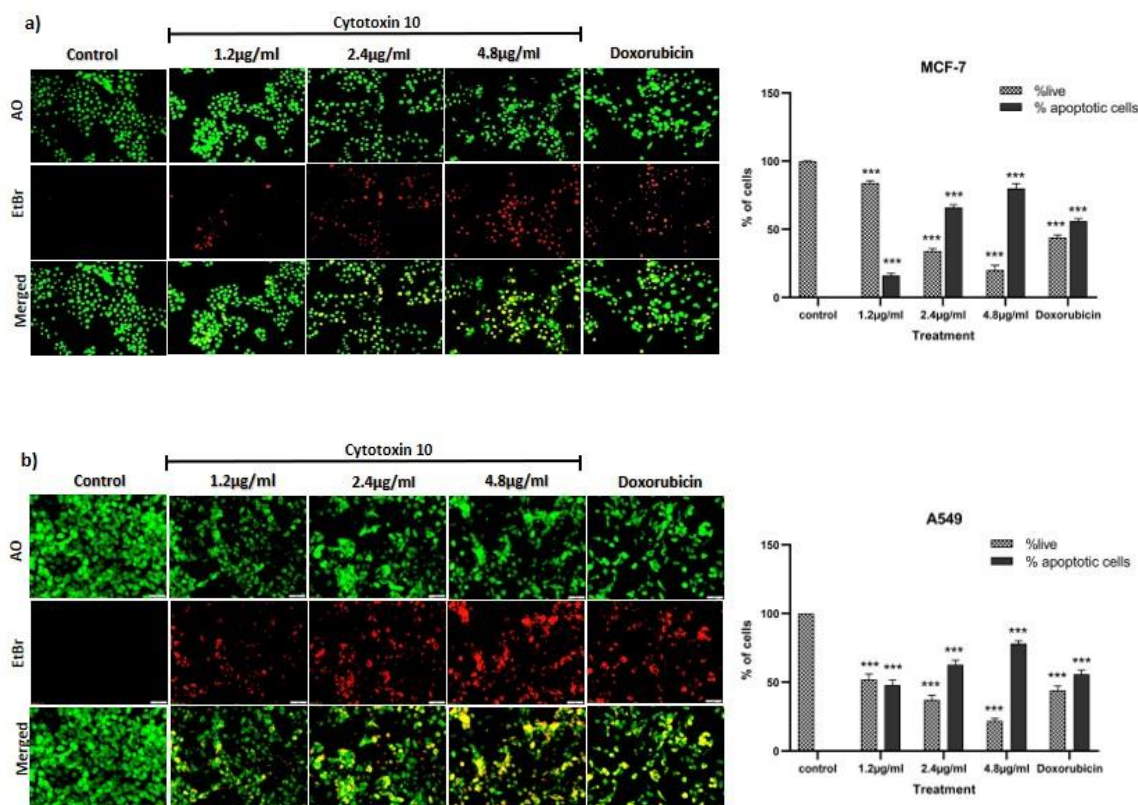


Figure 5.2: Dual Acridine Orange/Ethidium Bromide (AO/EtBr) staining of cancer cells visualized under a fluorescent microscope to check induction of apoptosis by Cytotoxin 10: AO/EtBr-stained images of a) MCF-7 cells after with Cytotoxin 10 for 48 hour and quantification of live and apoptotic cells. b) A549 cells stained with AO/EtBr and quantification after treatment with Cytotoxin 10 for 48 hour and quantification of live and apoptotic cells. Live (green), early apoptotic (yellow) and late apoptotic and/or necrotic cells (red) cells were counted manually. Statistical differences were analyzed with one-way ANOVA test. P value ***<0.05 was considered significant.

5.4.2.2 Annexin V-Alexa Fluor 488/PI binding study (FACS)

In MCF-7 cells, dual staining with Annexin V (Alexa Fluor 488)/ Propidium Iodide (PI) showed increase in early apoptotic cells (42%) when treated with low dose (1.2 µg/ml) of the purified protein (Figure. 5.3). However, treatment with higher doses (2.4 and 4.8 µg/ml) led to an increase in late apoptotic cells to ~31% and 57% respectively (Figure. 5.3). Cytotoxin 10 treatment of A549 cells suggested a dose dependent increase in late apoptotic cells. Treatment with doses of 2.4 and 4.8 µg/ml led to an increase in late apoptotic cells to about 37.3% and 64.4% respectively (Figure. 5.3). Furthermore, to understand the signaling mechanism leading to venom-induced apoptosis in both the cell

lines, expression level of apoptosis regulating proteins like Bax, Bcl-2, PARP, and caspase-7 was assessed and studied by western blotting.

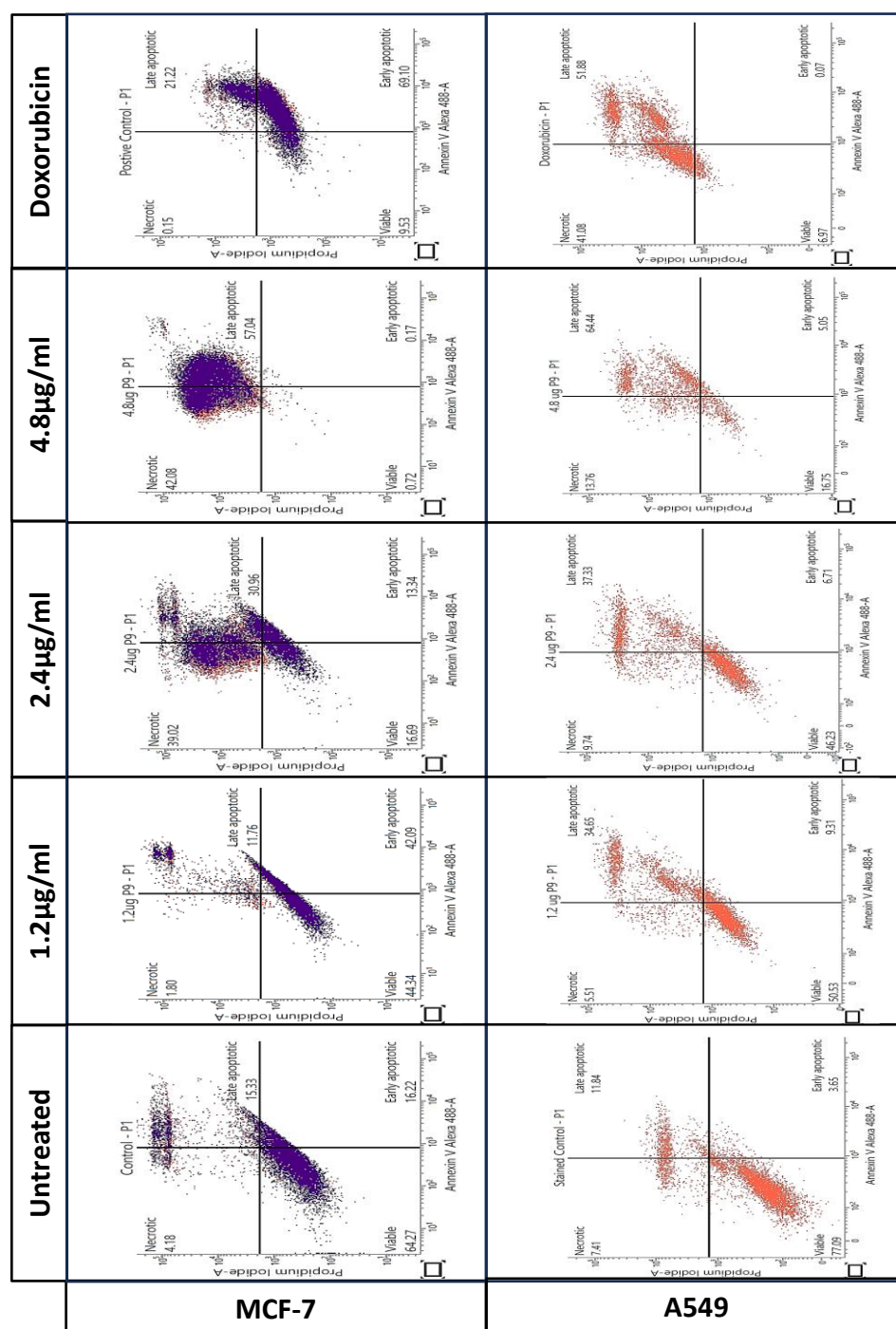


Figure 5.3: Flow cytometric analysis to understand the Cytotoxin 10-mediated cell death in breast (MCF-7) and lung (A549) cancer cell lines. Cells were stained with Annexin-V and/or Propidium Iodide. Non-treated cells were used as negative control and cells treated with Doxorubicin (1 µg/ml) treated cells were considered as positive control for the study.

5.4.3 Western blot analysis of apoptosis-associated proteins

To study the expression of the apoptosis-associated proteins, e.g. Bax, Bcl-2, caspase-7, PARP and p53 in Cytotoxin 10-treated MCF-7 and A549 cells, western blotting was performed. The IC₅₀ value of Doxorubicin is reported to be 1 µg/ml [331]. Therefore, 1 µg/ml dose was chosen as the positive control to confirm apoptosis induction.

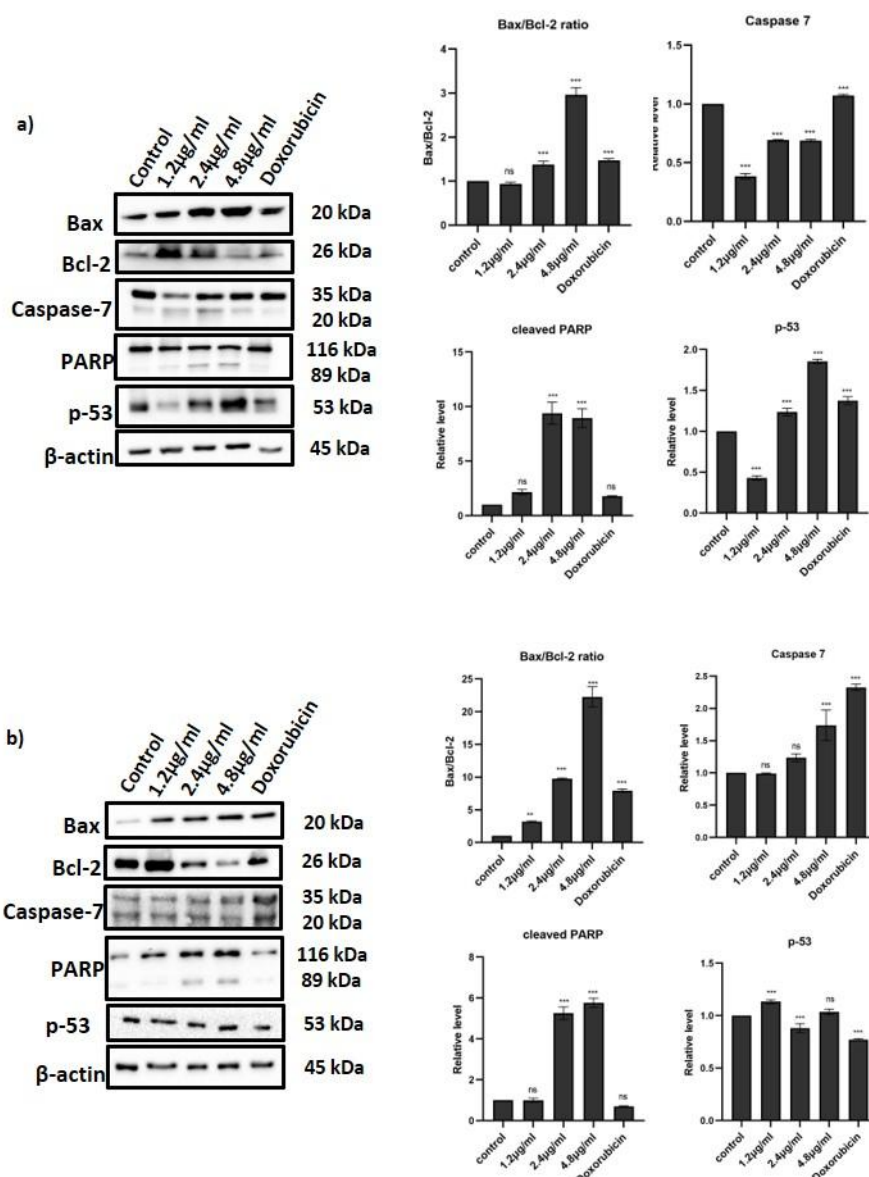


Figure 5.4: Western blot analysis of lysates from a) MCF-7 and b) A549 cells in response to *in vitro* treatment with Cytotoxin 10 (1.2 µg/ml, 2.4 µg/ml, 4.8 µg/ml) for 24 hours. Protein expression of apoptosis-associated proteins (Bax, Bcl-2, Caspase-7, PARP) and p-53 were analyzed. The ratio of Bax/Bcl-2, Caspase-7 expression and PARP cleavage after normalization with β-actin are presented in right panels. Cells treated with Doxorubicin (1µg/ml) was considered as positive control for the study. Statistical differences were analyzed with one-way ANOVA test and P-value <0.05 was considered significant.

Cytotoxin 10 induced expression of pro-apoptotic protein Bax and inhibited expression of Bcl-2 leading to increase in Bax/Bcl-2 ratio in both the cell lines, a marker that indicates induction of apoptosis (Figure. 5.4). The expression of caspase-7 along with its cleavage increased steadily in a concentration dependent manner. PARP cleavage with two bands corresponding to 116 kDa and 89 kDa was also observed after Cytotoxin 10 treatment. Tumor suppressor protein, p53 is expressed to regulate uncontrolled cell division and proliferation of cells. Cytotoxin 10 treatment of MCF-7 cells led to a dose-dependent increase in expression of p53 protein in MCF-7 cells. However, no significant change in p53 expression was observed in Cytotoxin-10 treated A549 cells suggesting p53 pathway independent anti-cancer activity.

5.4.4 Cytotoxin 10 inhibits migration and adhesion of cancer cells

To understand if Cytotoxin 10 affect the metastatic property of cancer cells, migration and adhesion assays were performed. Cytotoxin 10 at a dose of 0.6 and 1.2 $\mu\text{g/ml}$ inhibited migration of cells significantly. The wound area was significantly decreased in untreated MCF-7 after 24 and 48 hours (51.62% and 25.21%) respectively (Figure. 5.5a). However, wound area in 0.6 $\mu\text{g/ml}$ Cytotoxin 10-treated MCF-7 cells remained high at 24 hours (72.46%) and 48 hours (70.29%). Similar observation was noted in cells treated with 1.2 $\mu\text{g/ml}$ Cytotoxin 10 at 24 hours (75.91%) and 48 hours (73.60%). Similarly, in untreated A549 cells, the wound area was significantly decreased after 24 and 48 hours (52.76% and 20.87%) respectively (Figure. 5.5b). However, wound area in 0.6 $\mu\text{g/ml}$ Cytotoxin 10-treated A549 cells remained high at 24 hours (85.21%) and 48 hours (82.97%). Cells treated with 1.2 $\mu\text{g/ml}$ Cytotoxin 10 at 24 hours (86.81%) and 48 hours (84.72%) also showed higher wound width, suggesting a migration inhibiting activity of the protein.

Pre-treatment of the cells with various doses of Cytotoxin 10 led to inhibition of adhesion in MCF-7 and A549 cells. In MCF-7 cells, the percentage of adhered cells decreased dose-dependently from 82.55% (1.2 $\mu\text{g/ml}$) to 11.38% (4.8 $\mu\text{g/ml}$) after treatment with Cytotoxin 10. (Figure. 5.5c).

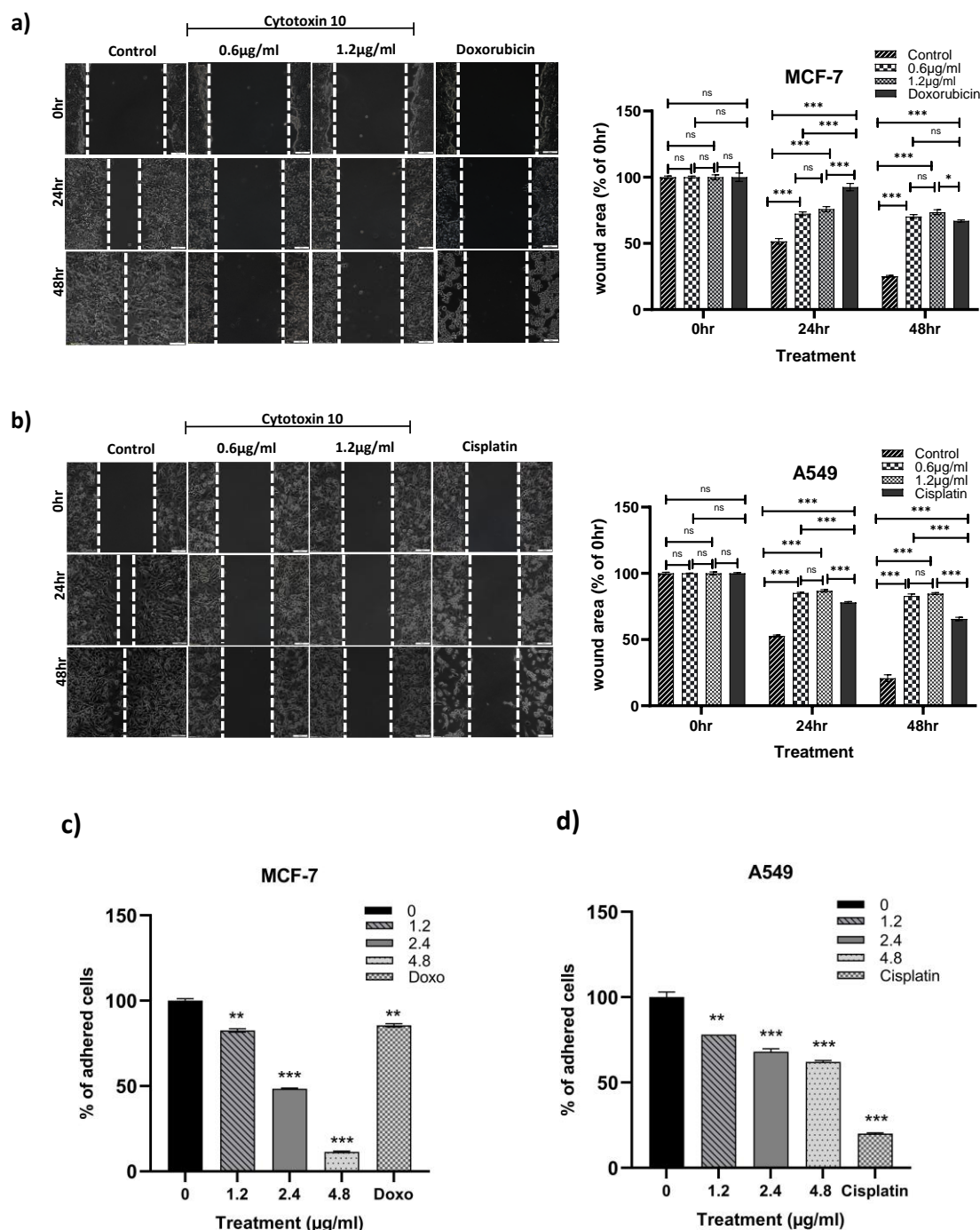
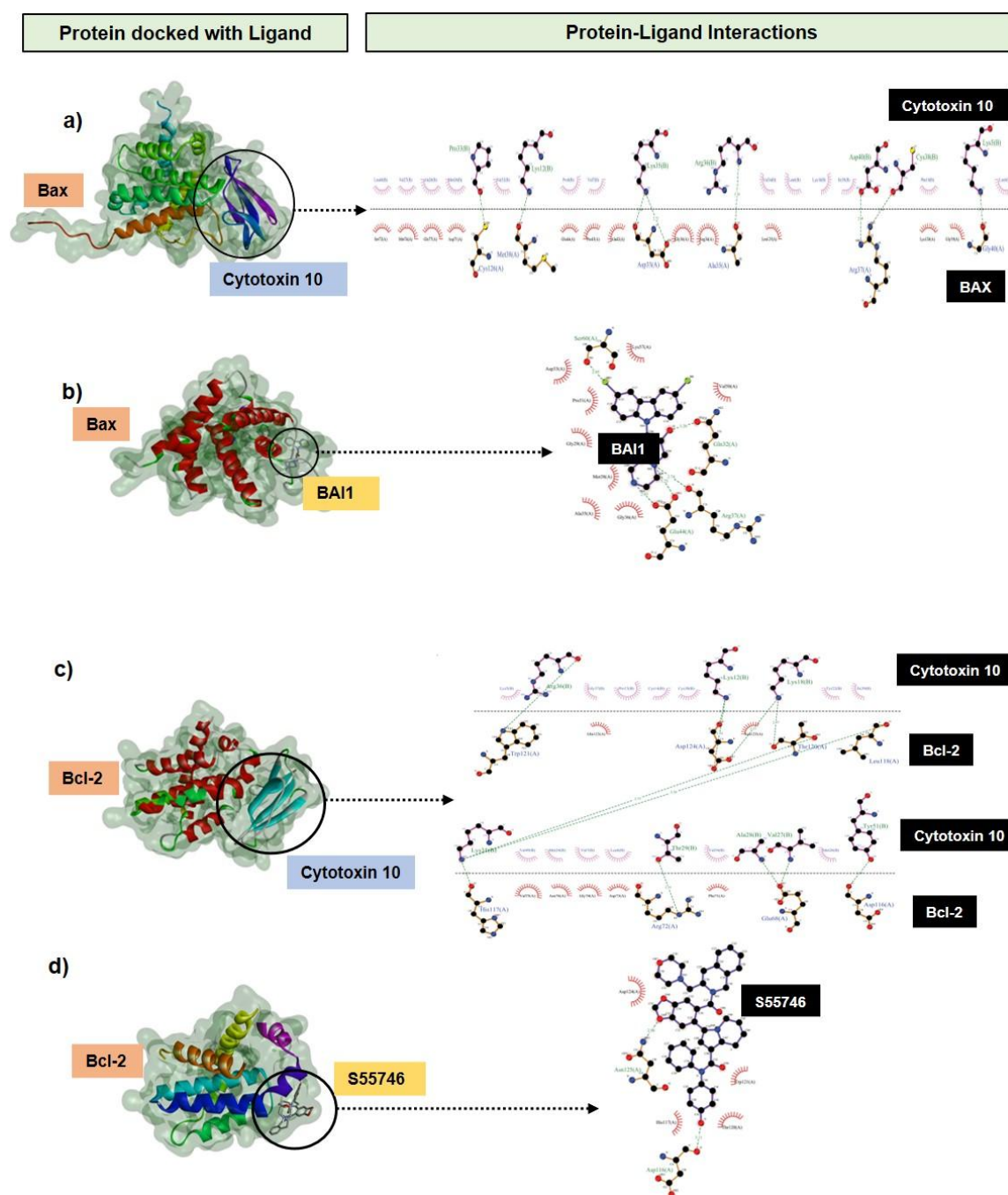


Figure 5.5: The effects of Cytotoxin 10 on migration and adhesion of breast (MCF-7) and lung (A549) cancer cells. Cells were treated with different doses of Cytotoxin 10 (1.2 µg/ml and 2.4 µg/ml). Wound width of a) MCF-7 and b) A549 cells after Cytotoxin 10 treatment (statistical analysis by two-way ANOVA test. P value ns > 0.05, * < 0.01, ** < 0.001, *** < 0.0001). Migration of cells were recorded at 24 and 48 hours. Inhibition of adhesion of cancer cells to collagen IV coated wells after 48hr treatment. % of adhered cells of c) MCF-7 cells and d) A549 in response to Cytotoxin 10 treatment (statistical analysis by one-way ANOVA test. P value ns > 0.05, * < 0.01, ** < 0.001, *** < 0.0001). Doxorubicin (1 µg/ml) and Cisplatin (50 µM) treated cells were taken as positive control for MCF-7 and A549 cells respectively for the study.

Similar observation was noted when A549 cells were treated with different doses of Cytotoxin 10. The percentage of adhered cells decreased significantly from 78.43% (1.2 µg/ml) to 61.63% (4.8 µg/ml) respectively (Figure. 5.5d).

5.4.5 Interaction studies of Cytotoxin 10 and apoptotic proteins

To elucidate the interactions of Cytotoxin 10 with Bax, Bcl-2, PARP1, and caspase-7, molecular docking analysis were performed. Comparative docking studies with established inhibitors of these proteins were also carried out. The statistics for the top 10 clusters from the HADDOCK server were reviewed for selection and the cluster exhibiting the lowest Z-score was selected for further analysis. Cytotoxin 10 displayed docking scores of -71.9 ± 10.1 , -89.2 ± 6.8 , -110.4 ± 3.5 , and -81.4 ± 4.8 with Bax, Bcl-2, PARP1, and caspase-7 proteins respectively. In contrast, Bax inhibitor BAI1, Bcl-2 inhibitor S55746, PARP1 inhibitor Olaparib, and caspase-7 inhibitor DICA showed docking score of -51.7 ± 2.3 , -38.6 ± 1.0 -24.7 ± 3.3 and -24.7 ± 0.6 respectively. This data suggested better efficacy of Cytotoxin 10 to interact with the target proteins compared to their specific inhibitors. The schematic representation of the interactions between target proteins and Cytotoxin 10 created using LigPlot+ are depicted in Figure. 5.6.



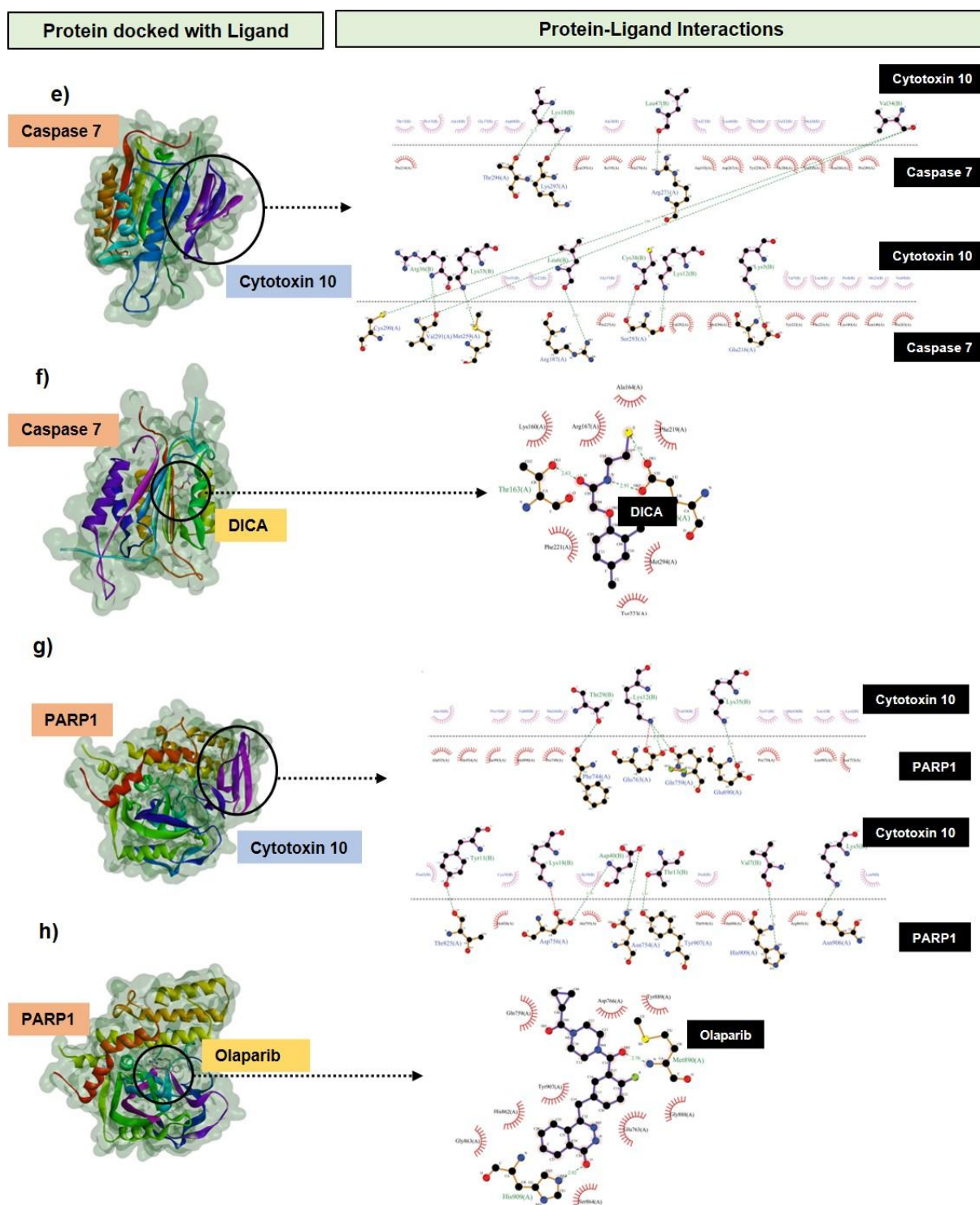


Figure 5.6: *In silico* interaction studies of active site of apoptotic proteins with Cytotoxin 10 compared to their corresponding known inhibitor obtained from HADDOCK server: a) Bax with Cytotoxin 10, b) Bax with BAI1, c) Bcl-2 with Cytotoxin 10, d) Bcl-2 with S55746, e) Caspase-7 with Cytotoxin 10, f) Caspase-7 with DICA, g) PARP1 with Cytotoxin 10, and h) PARP1 with Olaparib. The schematic representation of the interactions was illustrated using LigPlot+.

To confirm this observation, docking analysis was performed using another server HDOCK and the highest-scored conformation from the top 10 docked poses was selected for further evaluation. Cytotoxin 10 exhibited docking scores of -161.81 with Bax, -160.11 with Bcl-2, -163.82 with PARP1, and -119.84 with caspase-7. Among the inhibitors, BAI1 demonstrated a docking score of -80.28 with Bax, while S55746, Olaparib and DICA showed scores of -119.55, -145.31 and -82.61 with their respective proteins. This analysis also confirmed that Cytotoxin 10 had higher docking scores with the target proteins compared to their inhibitors. The interactions between the target proteins and Cytotoxin 10, illustrated using LigPlot+ are shown in Figure. 5.7. Comparative docking scores of Cytotoxin 10 and the inhibitors with the target proteins obtained from HADDOCK and HDOCK servers are summarized in Table 5.1.

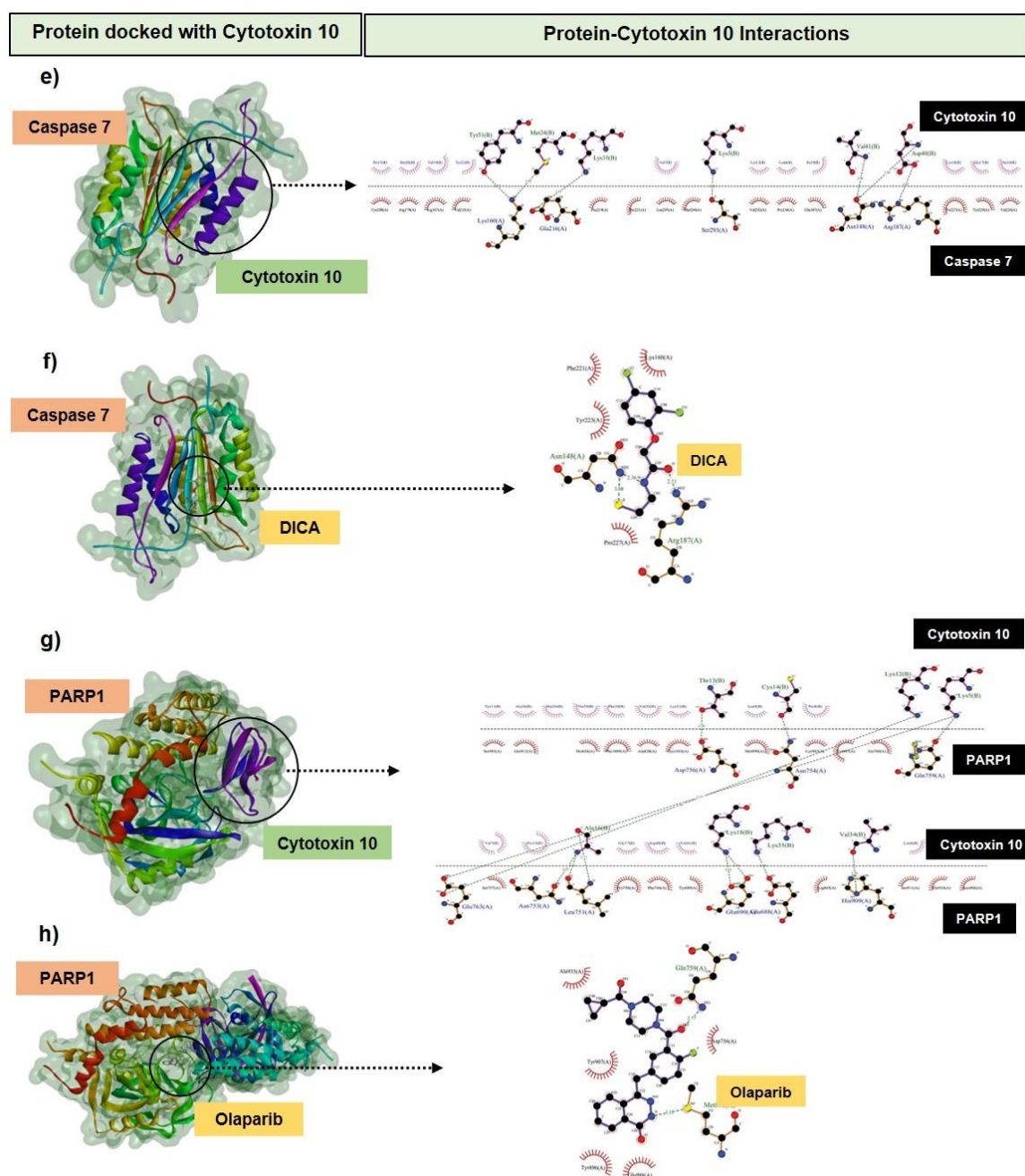


Figure 5.7: *In silico* interaction studies of active site of apoptotic proteins with Cytotoxin 10 compared to their corresponding known inhibitor obtained from HDock server: a) Bax with Cytotoxin 10, b) Bax with BAI1, c) Bcl-2 with Cytotoxin 10, d) Bcl-2 with S55746, e) Caspase-7 with Cytotoxin 10, f) Caspase-7 with DICA, g) PARP1 with Cytotoxin 10, and h) PARP1 with Olaparib. The schematic representation of the interactions was illustrated using LigPlot+.

Table 5.1: Interaction of Cytotoxin 10 and target proteins and target proteins with their inhibitors obtained from HADDOCK and HDock servers.

Target protein	Cytotoxin 10/ inhibitors	HADDOCK score	HDock score
BAX	Cytotoxin 10	-71.9 +/- 10.1	-161.81
	BAI1	-51.7 +/- 2.3	-80.28
Bcl-2	Cytotoxin 10	-89.2 +/- 6.8	-160.11
	S55746	-38.6 +/-1.0	-119.55
PARP1	Cytotoxin 10	-110.4 +/- 3.5	-163.82
	Olaparib	-24.7 +/- 3.3	-145.31
Caspase 7	Cytotoxin 10	-81.4 +/- 4.8	-119.84
	DICA	-24.7 +/- 0.6	-82.61

5.5 Discussion

Snake venom is a complex mixture of proteins and peptides which induces diverse pharmacological effects including anti-cancer activity. Extensive literature survey has suggested that cytotoxins from Elapid venom can induce cell death *via* apoptosis in both *in vitro* and *in vivo* studies. For instance, cytotoxins from *N. naja* venom inhibited human leukemic U937 cell growth by inducing apoptosis and arresting cell cycle [292]. Cytotoxin-II isolated from the Caspian cobra was also reported to induce apoptosis in MCF-7 cell line [293]. Cytotoxin isolated from *Bungarus fasciatus* induced cell death in both *in vitro* (leukemic cell line U937) and *in vivo* (EAC induced BALB/c mice) conditions *via* apoptosis by downregulating PI3K/Akt and MAP-kinase pathways [318].

This chapter describes the mechanism of cytotoxic activity of Cytotoxin 10 purified from *N. kaouthia* from North-East India origin against breast and lung cancer cell lines. The effect of Cytotoxin 10 on the morphology of breast and lung cancer cells suggested that Cytotoxin 10 induces a concentration-dependent cell death in both breast and lung cancer cells which correlates to the findings of the cell viability (MTT) assay. To ascertain the potential involvement of apoptosis in cell death, fluorescence microscopy was performed using AO/EtBr staining [332]. Cytotoxin 10 treated cells led to a significant increase in apoptotic cells in a concentration-dependent manner. Further validation was done using flow cytometry analysis using Annexin V/PI dual staining, which revealed a similar concentration-dependent increase in apoptotic cells in both MCF-7 and A549 cells [207].

MCF-7 cells treated with the lowest dose exhibited early apoptotic cell death, however, further increase in dosage led to late apoptotic cell death. These findings correspond with the study of cytotoxin (NK-CT1) treatment in leukemic cell lines (U937 and K562) showing both early and late apoptosis as the mechanism of cell death [241]. However, Cytotoxin 10 treatment of A549 cells suggested a dose-dependent increase in the late apoptotic cell death. Similar findings were reported earlier by Chong and his co-worker with cytotoxin isolated from *N. kaouthia* (Thailand) [289]. Cytotoxins from other *Naja* species have also demonstrated late apoptosis in lung cancer, breast cancer and leukemic cell lines [293] [241].

Apoptosis is a critical hallmark of cell death, and hence, the expression of apoptosis related proteins in Cytotoxin 10 treated cells were studied. Bax interacts with mitochondrial voltage dependent anion channel leading to loss of membrane potential and release of cytochrome c followed by activation of caspases. Two types of caspases namely initiator and executioner caspases play significant roles in apoptosis [333,334]. Activated Caspases cleave substrates, including PARP for execution of apoptosis. Cytotoxin 10 treatment induced the expression of pro-apoptotic protein Bax, and inhibited the expression of an anti-apoptotic protein Bcl-2, leading to an increase in Bax/Bcl-2 ratio, an indicator of apoptotic cell death. This observation was supported by induction of caspase-7 expression and cleavage of PARP suggesting Cytotoxin 10-induced apoptosis in both MCF-7 and A549 cell lines. Expression of Bax is regulated by p53. Cytotoxin 10 treatment increased expression of p53 protein in MCF-7 cells suggesting p53-induced apoptosis. p53 protein is a tumor suppressor that plays a critical role in DNA repair, cell cycle regulation and apoptosis. In response to cellular stress, p53 is activated, leading to cell cycle arrest, DNA repair or apoptosis. The MCF-7 breast cancer cell line expresses wild-type p53 suggesting that it can carry out its normal tumor suppressing functions [335,336]. It has been reported that p53 function can be manipulated in MCF-7 cells [337]. Further, the status of p53 also influences cell sensitivity to certain treatments [335,338].

Snake venom has the potential to induce p53 expression by causing cellular stress or DNA damage in MCF-7 cells, leading to various cellular responses, including apoptosis [339]. Ruviprase, a small peptide from *Daboia russelii russelii* venom induced apoptosis in MCF-7 cells through p53 and p21-mediated pathways [340].

Under normal, unstressed conditions, p53 protein is maintained at low intracellular levels due to its rapid degradation, resulting in a short half-life. This regulation is primarily mediated by the Mdm2 oncoprotein, which targets p53 for ubiquitination and subsequent proteasomal degradation [341,342]. However, in response to cellular stress, such as DNA damage, p53 becomes stabilized through posttranslational modifications that inhibit its interaction with Mdm2. This stabilization allows p53 to accumulate and activate the transcription of genes involved in cell cycle arrest or apoptosis [342]. In this study, increased p53 expression in MCF-7 cells might be observed due to cellular stress induced following Cytotoxin 10 treatment. The protein might be able to interact and stabilize p53, inducing apoptosis.

Molecular docking studies provided critical information on the interactions of Cytotoxin 10 with apoptosis-associated proteins Bax, Bcl-2, PARP1 and caspase-7. In comparison to the known inhibitors of these proteins, Cytotoxin 10 showed consistently higher binding scores. This suggests that Cytotoxin 10 could potentially bind to the apoptosis-related proteins for modulation of their expression leading to apoptosis-induced cell death in both breast and lung cancer cells.

Previous studies have reported that cytotoxins may activate different pathways for programmed cell death. For instance, cytotoxins may induce Ca^{2+} influx leading to increased levels of Ca^{2+} in the cytosol which induces apoptosis *via* the Ca^{2+} /protein phosphatase 2A (PP2A)/adenosine monophosphate protein kinase (AMPK) pathway [343]. Similarly, cytotoxins may promote reactive oxygen species (ROS) generation in cells resulting in apoptosis [344]. Moreover, cytotoxins may also induce apoptosis by upregulating proapoptotic mediators like Bax, Bad and endonuclease G, and downregulating X-linked inhibitor of apoptosis protein (XIAP), Bcl-XL, Bcl-2, Mcl-1 and survivin. Along with these mediators, cytotoxins also promote apoptosis by inhibiting the phosphatidylinositol 3-kinase (PI3K)/Akt, Epidermal growth factor receptor (EGFR), and Janus tyrosine kinase 2 (JAK)/ signal transducer and activator of transcription 3 (STAT3) pathways [345-347].

Metastasis is an important characteristic acquired by the malignant cancer cells and it involves processes like migration and adhesion of these cells [348]. Migration of cancer cells from primary site to distant sites is an integral event of initiation of metastasis. Previously, snake venom proteins including SVMPs, disintegrins, C-type lectins, LAAOs have been reported to inhibit metastasis in cancer cells [225,349-352]. Therefore, the influence of Cytotoxin 10 on migration and adhesion of breast and lung cancer cells was explored in this study. Wound healing assay suggested that Cytotoxin 10 treatment inhibits migration in both breast (MCF-7) and lung (A549) cancer cell lines in a dose-dependent manner. Another 3FTx, Cardiotoxin III isolated from *N. atra* venom has also been reported to inhibit migration in oral (Ca9-22) cancer cells *via* downregulation of MMP-2/-9; phosphorylation of JNK and p38-MAPK pathways [353]. In this study, Cytotoxin 10 also dose-dependently inhibited adhesion of cancer cells to collagen IV. Collagen IV protein is a crucial component of the basement membrane which is a dense layer of ECM. Collagen IV plays a vital role in various cellular functions like adhesion, migration, proliferation and cell survival [354]. It forms a heterotrimer consisting of three α -chains, each of which consists of an amino-terminal, a collagenous, and a carboxyl-end non-collagenous domains [355]. Collagen IV interacts with other components of the ECM (proteoglycans, laminins, etc) and also with cellular receptors like integrins, thus providing structural support to the cells and helps in adhesion and migration of the cells [354]. Therefore, inhibition of adherence of cancer cells to Collagen IV by Cytotoxin 10 suggests its potential role in anti-metastatic activity. Other venom proteins like SVMPs have also been reported to inhibit endothelial cell adhesion *via* degradation of ECM proteins like fibronectin, vitronectin, collagen I & IV and plasma proteins [188,356,357].

Snake toxins have been reported to inhibit signals promoting migration and invasion of cancer cells which are activated by the ECM proteins (collagen, laminins, etc) and various growth factors like epidermal growth factor (EGF), transforming growth factor beta (TGF- β), etc *via* 3 types of mechanism. First type includes inhibition of adhesion and migration which are dependent on ECM proteins: snake venom disintegrins, C-type lectin-like protein and KSPI interacts with integrins in cancer cells to exhibit anti-metastatic activity [225,358,359]. The second type includes resistance to epithelial-mesenchymal transition (EMT). EMT involves downregulation of E-cadherin which is

an epithelial marker but upregulation of vimentin and N-cadherin which are the mesenchymal markers; and MMP-2/-9 [360]. Cardiotoxin III inhibits the EGF-induced migration and invasion in cancer cells by inhibiting EMT *via* EGFR-dependent PI3K/Akt, ERK1/2 and NF- κ B signaling thus down-regulating MMP-2/-9 expressions [201,353,361]. The third type includes inhibition of metastasis by altering the actin/cytoskeleton network: Daboialectin isolated from *D. russelii* venom was reported to alter morphology of A549 cells *via* cytoskeletal changes through RHO-GTPases, thus inhibiting adhesion and invasion [362]. Also, BJcuL isolated from *B. jararacussu* venom induced apoptosis in human gastric carcinoma cells along with disassembly of actin cytoskeleton and cell adhesion inhibition [222].

The cytotoxins are one of the most abundant proteins in cobra venom and different types of cytotoxins may be present in a single cobra venom all of which share a similar three-finger fold spatial structure [307,363,364]. The occurrence of large number of hydrophobic amino acids in cytotoxins along with formation of a uniform hydrophobic platform indicate that it may interact with lipid membranes [365]. The hydrophobicity depends on the presence of either Ser29 (S-type cytotoxins) or Pro31 (P-type cytotoxins) and it has been determined that S-type cytotoxins are less hydrophobic than the P-type cytotoxins [366,367]. Moreover, cytotoxins also have other extended surfaces apart from the membrane binding motif which enable them to interact with heparin-oligosaccharides and derivatives of ATP [368]. Interaction of cytotoxin with carbohydrate domains of proteoglycans or syndecans may assist in their internalization into cells where they may affect cell organelles such as mitochondria or lysosomes. It has been hypothesized that inside the cell, the cytotoxins may compete with anionic lipid membranes displacing them to the cytoplasm which may act as a trigger for apoptosis [73].

This chapter suggested that Cytotoxin 10 isolated from *N. kaouthia* venom induces cell death in cancer cells *via* the mechanism of apoptosis and it was also observed that Cytotoxin 10 inhibited the metastatic properties of cancer cells. Thus, the current findings extended our understanding of *in vitro* cytotoxic effect of the snake venom protein Cytotoxin 10 against human breast and lung cancer cells.

Based on the results of the experiments, we propose a model on the mechanism of cell death induced by Cytotoxin 10 in cancer cells (Figure 5.8). The proposed mechanism of apoptotic cell death involving mediators of the intrinsic and extrinsic pathways are illustrated in the proposed model. In both the pathways, activation of the effector caspase-3 and caspase-7 occurs which leads to apoptosis.

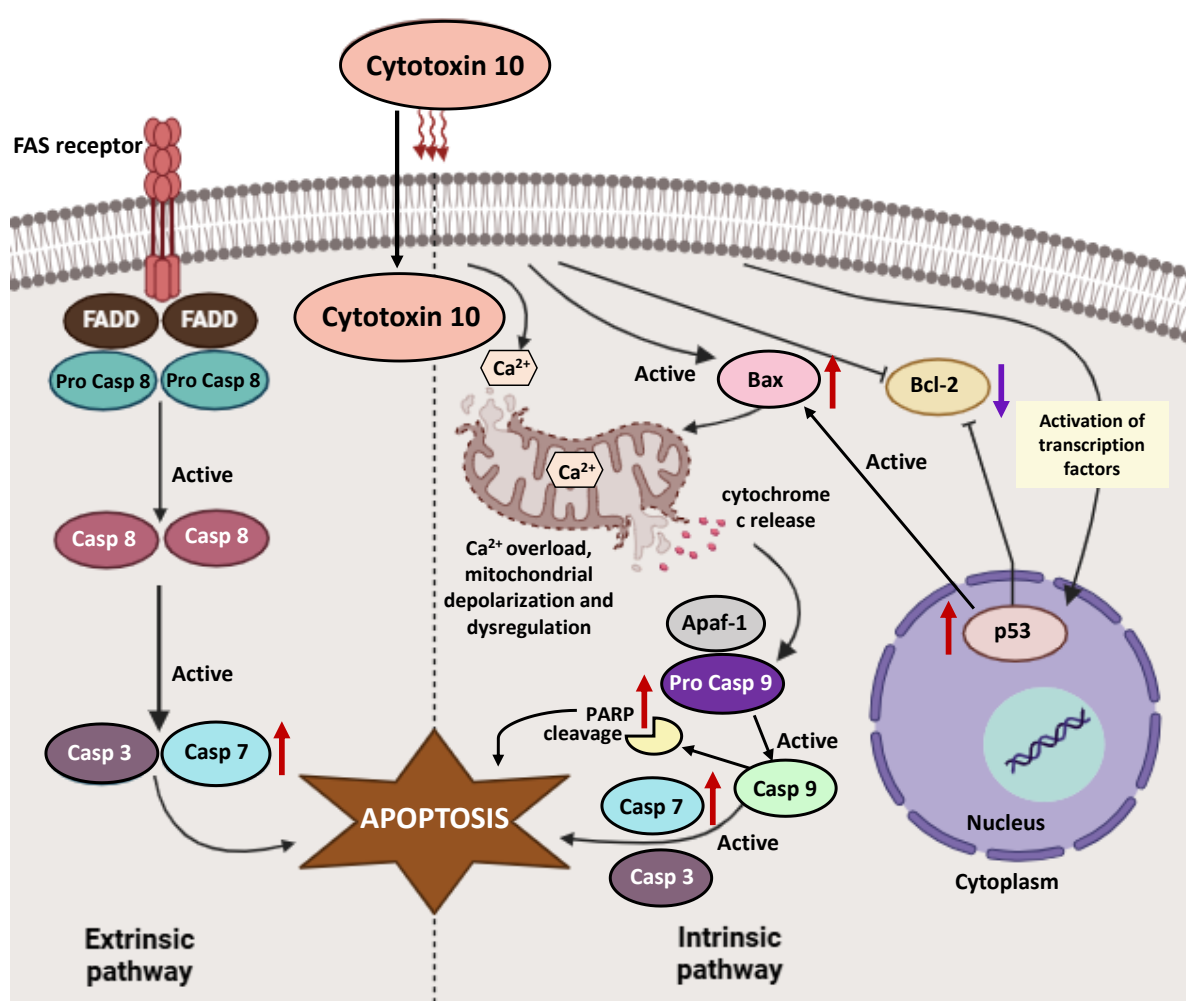


Figure 5.8: Proposed mechanism of apoptotic cell death induced by Cytotoxin 10. Blue arrow represents downregulation and red arrow represents upregulation of apoptosis-associated proteins. The model is drawn using BioRender software.